

# Atomistic simulations of the LaMnO<sub>3</sub> (110) polar surface

E. A. Kotomin,<sup>\*ab</sup> E. Heifets,<sup>ac</sup> J. Maier<sup>a</sup> and W. A. Goddard III<sup>c</sup>

<sup>a</sup> Max Planck Institut für Festkörperforschung, Heisenbergstr. 1, D-70569 Stuttgart, Germany.  
E-mail: kotomin@fkf.mpg.de

<sup>b</sup> Institute for Solid State Physics, University of Latvia, 8 Kengaraga, LV-1063 Riga, Latvia

<sup>c</sup> Materials and Process Simulation Center, Beckman Institute, California Institute of Technology, MS 139-74, Pasadena, CA 91125, USA

Received 10th July 2003, Accepted 21st August 2003

First published as an Advance Article on the web 4th September 2003

The results of atomic structure calculations, with a focus on the surface relaxation and polarization, are presented for the LaMnO<sub>3</sub> (110) O-terminated polar surface. We compare results of the classical shell model calculations for four possible terminations, including (1 × 2) (110) surface reconstruction, and demonstrate that the latter has the lowest surface energy. The surface energy is saturated only when six to eight near-surface atomic planes are relaxed which is accompanied by the considerable dipole moments perpendicular to the surface. Results are compared with those for iso-structural BaTiO<sub>3</sub> (110) surfaces.

## I. Introduction

Thin ABO<sub>3</sub> perovskite films are important for many technological applications, including ferroelectric memories, catalysis, chemical sensors, microelectronics, substrates for growth of high  $T_c$  superconductors *etc.*<sup>1,2</sup> In particular, LaMnO<sub>3</sub> is of great interest as a cathode material for fuel cell applications (see, *e.g.*<sup>3</sup>) as well as a magnetoresistive device material, due to the CMR effect.<sup>4</sup> Several *ab initio* quantum mechanical<sup>5–14</sup> and classical shell model (SM)<sup>15–20</sup> theoretical studies were published recently for the (100) surfaces of BaTiO<sub>3</sub> and SrTiO<sub>3</sub> crystals. As far as transition-metal perovskites are concerned, we are familiar with only two calculations of the (100) surfaces: CaMnO<sub>3</sub> and La<sub>0.5</sub>Ca<sub>0.5</sub>MnO<sub>3</sub>, with a focus on their magnetic properties.<sup>21</sup> To our knowledge, there exist no calculations for the LaMnO<sub>3</sub> surfaces. Unlike the above-mentioned perovskites, the LaMnO<sub>3</sub> (100) surface is unstable since it consists of a sequence of alternating charged planes (LaO, MnO<sub>2</sub>) which produces an infinite dipole moment perpendicular to the surface.<sup>22</sup> This should result in a reconstruction of a flat surface involving formation of steps, kinks *etc.* Another, flat LaMnO<sub>3</sub> surface is the (110) O-terminated surface which is iso-structural to the SrTiO<sub>3</sub> and BaTiO<sub>3</sub> (110) surfaces. Only a few semi-empirical quantum mechanical calculations<sup>23,24</sup> have been performed for the perovskite (SrTiO<sub>3</sub>) (110) surfaces. We also performed recently SM calculations on the atomic relaxation for the polar (110) surfaces of SrTiO<sub>3</sub>, BaTiO<sub>3</sub><sup>20,25</sup> and KNbO<sub>3</sub>.<sup>26</sup> We present the results of the first calculations of the atomic structure of the flat LaMnO<sub>3</sub> (110) surface.

## II. Methods and surface models

Keeping in mind the fuel cell applications, we restrict ourselves to simulations of LaMnO<sub>3</sub> in its cubic crystalline phase stable at high temperatures ( $T \geq 800$  K). This is why one can neglect the Jahn–Teller and other delicate effects, well studied for the LaMnO<sub>3</sub> bulk at low temperatures,<sup>27,28</sup> and focus on the surface relaxation. The SM model and its parameterization are described in detail in refs. 20, 29–31. Note here only that

in the SM the interatomic interactions are described by the core-core, core-shell and shell-shell pair potentials. In this approach, each ion has a charged core and the electronic shell. The sum of the core and shell charges gives the formal charge of the corresponding ion. The spring  $k$  connects the core and the shell of the same ion. The core-shell separation is a measure of the *atomic polarization*. The interactions between cores and shells of different ions are Coulombic whereas the interactions between the shells of different ions contain also the short-range potentials accounting for the effects of the exchange repulsion and the van-der-Waals attraction. The Buckingham potentials with three parameters per pair of atoms are widely used for the short-range interactions (see below). To study the surface relaxation, we optimize the atomic positions in several (varied from one to 16) near-surface planes, placed into the electrostatic field of the substrate. The latter is simulated by a number of additional planes whose atoms are fixed in the perfect lattice sites. The number of this planes was chosen to reach a convergence of the crystalline field in the surface planes. 2D Ewald summation of the Coulombic interactions is applied.

Use of this model permits us to find the atomic relaxation for several hundreds of atoms, surface energies, along with the surface polarization, characterized by dipole moments perpendicular and parallel to the surface. This information is of great importance for analysis of ferroelectric properties of thin ferroelectric films and their reactivity. We allow atoms in a given number of near-surface planes to relax to the minimum of total energy, and then analyze, how the major properties are affected by a number of relaxed planes. This is important since in time-consuming *ab initio* calculations only two to three near-surface planes are typically allowed to relax. Calculations are performed using the MARVINS computer code.<sup>32</sup> This code has been widely and successfully used for the atomistic modelling of complex ionic surfaces in the framework of the slabs infinite in two dimensions.

The well-known problem of modelling the (110) polar surface arises from the fact that it consists of charged planes. If the (110) surface were to be modelled exactly as one would expect after crystal cleavage, it would have an *infinite* dipole moment perpendicular to the surface, which makes such a

surface unstable.<sup>1,22</sup> (This was mentioned already with respect to the  $\text{LaMnO}_3$  (100) surface.) To avoid this problem, in our calculations we removed half the O atoms from the O-terminated surface. As a result, we obtain the (110) surface with charged planes but a zero dipole moment (before atomic relaxation). The relevant surface cells are built from neutral five-atom elements from three successive planes which are shown as bold encircled dashed ellipses in Fig. 1. It should be noted here that, in principle, the polar surface could be also stabilized due to the charge transfer between near-surface planes. However, CNDO calculations<sup>23</sup> indicate and *ab initio* calculations<sup>33</sup> confirm that the surface energy of such the  $\text{SrTiO}_3$  (110) exceeds considerably the surface energies of the above-mentioned terminations with removed atoms and is thus energetically unfavourable. The initial atomic configuration for the O-terminated surface, where every second surface O atom is removed and others occupy the same sites as in the bulk structure, we call asymmetrical (A in Fig. 1). Since such a removal of half of O atoms disturb the balance of interatomic forces along the surface, we also studied another, *symmetrical* initial surface configuration B in which the  $\text{O}_2$  atom is placed in the *middle* of the distance between two equivalent O atoms in the bulk. The A-type surface reveals considerable atomic displacements not only perpendicular to the surface, but also parallel to the surface. The results for the A and B cases for  $\text{SrTiO}_3$  and  $\text{BaTiO}_3$  have been discussed in ref. 20. Recently,<sup>25</sup> we suggested and studied for  $\text{SrTiO}_3$  and  $\text{BaTiO}_3$  another possible configuration C which corresponds to the  $(1 \times 2)$  surface reconstruction where O atoms are removed in pairs of nearest surface cells in a “zig-zag” way (the remaining  $\text{O}_2$  and  $\text{O}_3$  are

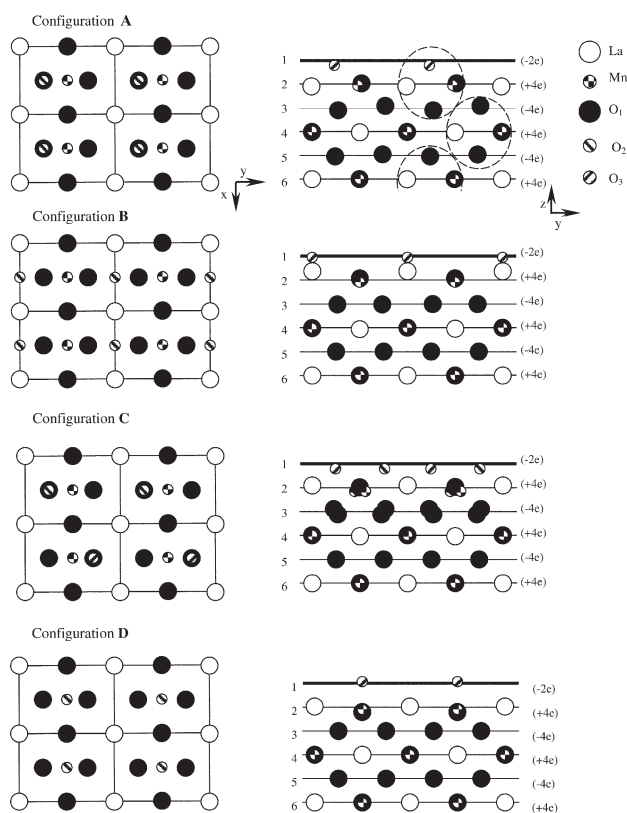


**Fig. 1** The top and front view of the (110)  $\text{LaMnO}_3$  surfaces. A to D are four possible configurations of the O-terminated surface, the outermost surface plane contains only  $\text{O}_2$  and  $\text{O}_3$  atoms whereas  $\text{O}_1$  atoms lie in the sub-surface plane. As one can see, in the configuration A atoms  $\text{O}_2$  sit above  $\text{O}_1$ , in the configuration C atoms  $\text{O}_2$  and  $\text{O}_3$  are above  $\text{O}_1$  of the second plane, and in the configuration D atoms  $\text{O}_2$  sit above the Mn atoms. Dashed ellipses containing five atoms from three nearest planes show neutral fragments from which the surface unit cells are built. The numbers in brackets on the right hand side of planes give the corresponding effective charges.

alternating in the nearest surface cells as shown in Fig. 1). In this case, in contrast to case A, there is no dipole moment parallel to the surface. Lastly, one more possible termination corresponds to  $\text{O}_2$  surface ions sitting atop  $\text{Mn}^{3+}$  ions (configuration D in Fig. 1) which seems intuitively to be energetically favourable.

We analyzed recently<sup>13,14</sup> atomic displacements in the (100) outermost  $\text{SrTiO}_3$  planes, obtained by means of various *ab initio* methods as well as SM calculations. In all calculations of the (100) surface, the energy corresponding to the SrO termination is only slightly smaller than for the  $\text{TiO}_2$  termination, both of the order of 1.2 eV per surface unit cell. Thus, both (100) surfaces can co-exist, in agreement with experimental observations.<sup>13</sup> The SM results were in very good agreement with *ab initio* calculations.

Several SM calculations were performed on the bulk defects in  $\text{LaMnO}_3$ <sup>29–31</sup> using different parameterizations. We used here the latest parameters<sup>4</sup> given in Table 1 which reproduce successfully the main  $\text{LaMnO}_3$  bulk properties (lattice constant, dielectric properties, three distinctive low frequency TO phonons) and polarons therein (Table 2) (see discussion).<sup>4</sup> Note here only that La and Mn atoms, unlike O atoms, have no electron shells and thus their polarization is neglected.

### III. Main results

Atomic relaxations of the first three top layers and four possible terminations (Fig. 1) are given in Table 3. For a comparison we present also results for  $\text{BaTiO}_3$ . The top O atoms on the asymmetrical surface termination A are considerably, by 8.2%, displaced inwards and polarized (the core-shell relative displacement is as large as 4.8%). The Mn atom in the second plane is displaced also inwards, by 1.7%. Along with the displacements along the  $z$ -axis perpendicular to the surface, all atoms on this surface reveal also considerable displacements *parallel* to the surface, along the  $y$ -axis. This produces the relevant dipole moments  $p_y$ , to be discussed below. Analysis of near-surface relaxation indicates the tetragonal anti-ferro-distortive (AFD) type-mode observed in the STO bulk below 105 K (ref. 1). This mode corresponds to the rotation of the  $\text{MnO}_6$  octahedra in nearest neighbour (NN) cells in the opposite directions. The rotation [001] axis is parallel to the surface. Results for the  $\text{BaTiO}_3$  (Table 3) agree qualitatively with those for the  $\text{LaMnO}_3$ ; directions of all atomic displacements are the same.

In contrast to the A-case, atoms on the symmetrical termination B are relaxed mostly along the  $z$  axis, due to symmetry reasons, and reveal much smaller displacements (*e.g.*, the top O atoms go inwards, by 1.8%, and strongly polarized.) The only small  $y$ -displacements occur for O atoms in the third plane. Note also that Ba atoms in the *second* plane of  $\text{BaTiO}_3$  were strongly displaced outwards the surface, unlike La in  $\text{LaMnO}_3$ . This difference arises due to a combination of different effective charges of  $\text{La}^{3+}$  and  $\text{Ba}^{2+}$ , and neglect of the electronic shell on La (see ref. 26 dealing with the cation polarization effects on the  $\text{KNbO}_3$  (110) surface).

The displacements of atoms in the top layers on the C-type surface are quite similar to those on the A-type surface. This surface also demonstrates the AFD type-mode. However, the

**Table 1** Parameters  $A$ ,  $\rho$  and  $C$  of Buckingham pair potentials, O shell charge  $Y$  and and the core-shell spring constant  $k$  (ref. 4) used in our  $\text{LaMnO}_3$  surface calculations

Ions	$A/\text{eV}$	$\rho/\text{\AA}$	$C/\text{eV \AA}^{-6}$	$Y/e$	$k/\text{eV \AA}^{-2}$
$\text{La}^{3+}\text{-O}^{2-}$	1516.3	0.3639	0.0		
$\text{Mn}^{3+}\text{-O}^{2-}$	1235.9	0.3152	0.0		
$\text{O}^{2-}\text{-O}^{2-}$	22764.3	0.1490	20.37	-2.48	16.8

**Table 2** Calculated and experimental crystal properties, including the lattice constant  $a_0/\text{\AA}$ , cohesive energy,  $E_{\text{coh}}/\text{eV}$ , dielectric constants, and three characteristic TO-phonon frequencies/ $\text{cm}^{-1}$

	$a_0$	$E_{\text{coh}}$	$\epsilon_0$	$\epsilon_\infty$	$\omega_{\text{TO1}}$	$\omega_{\text{TO2}}$	$\omega_{\text{TO3}}$
expt	3.89		$18 \pm 2$	4.9	172	360	560
theory <sup>4</sup>	3.89	-140.52	15.6	4.9	172	308	513

directions of octahedra rotations are *alternating* in NN cells *along* the rotation axis. (Note that in the A-case all these  $\text{MnO}_6$  octahedra are rotated in the same direction.) This is why due to the symmetry reasons the displacements of the La (Ba) and O ions in the even layers along the  $y$  axis are zero in Table 3. Lastly, calculations for the termination D demonstrate very strong surface O polarization (core-shell displacement of 7.2%) and considerable displacement of O atoms in the second plane.

Table 4 demonstrates considerable difference in the surface energies which are calculated allowing only two planes and all 16 near-surface layers to relax. (The surface energy for the unrelaxed A terminated surface is as large as 6.8 eV.) Fig. 2 shows additionally that the (110) surface energy saturates at about 6–8 relaxed layers only. This is in contrast with many *ab initio* calculations where only 1–2 layers are relaxed. Unlike the (100) perovskite surfaces, our four  $\text{LaMnO}_3$  (110) surface terminations strongly differ in energies. The  $(1 \times 2)$  reconstructed, “zig-zag” termination C turns out to be the lowest in energy (1.95 eV per surface cell). This is slightly lower than the A termination but about twice smaller than the symmetrical B termination (4.06 eV per cell) and the more so than the D termination, which turns out to be the energetically less favourable.

Fig. 3 shows the macroscopic (110) surface polarization, characterized by the relaxation-induced dipole moments (per surface unit cells)  $p_z$  and  $p_y$ , perpendicular and parallel to the surface, respectively. For the asymmetrical termination A the

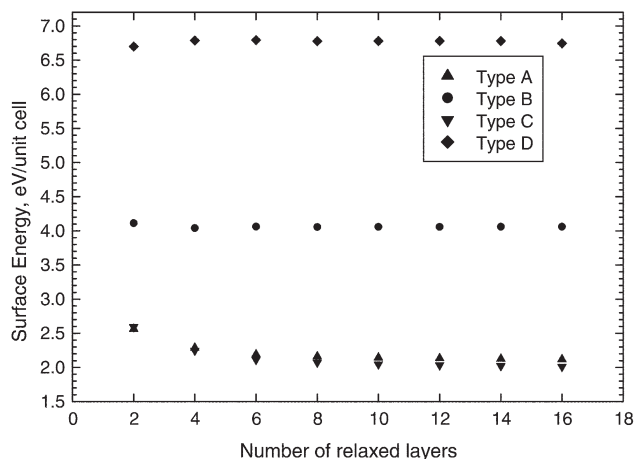


**Fig. 2** Surface energies for four terminations of the  $\text{LaMnO}_3$  (110) surfaces (Fig. 1) as a function of the number of relaxed near-surface planes.

surface polarization  $p_z$  oscillates around the limiting value of  $1 e \text{\AA}$ , as the number of relaxed near-surface planes increases from 2 to 16. This is accompanied by the considerable dipole moment  $p_y = 3.3 e \text{\AA}$  parallel to the surface, which also very slowly saturates. In contrast, the  $p_z$  dipole moment for the B termination rapidly saturates at  $0.77 e \text{\AA}$ , whereas  $p_y$  tends to zero, with an increase of a number of relaxed layers. Lastly, for the “zig-zag” termination C,  $p_z$  saturates at  $1.1 e \text{\AA}$  similarly to the asymmetrical case A but much faster and, by the symmetry reasons, the dipole moments parallel to the surface vanish. Lastly, the termination D shows the smallest polarization (but it is the most energetically unfavourable). In other words, the  $\text{LaMnO}_3$  surface relaxation produces a considerable polarization perpendicular to the surface which results from near-surface atomic relaxation. This could affect the molecular adsorption and reactions on the  $\text{LaMnO}_3$  surfaces.

**Table 3** Atomic relaxation of three top layers (in percent of the lattice constant,  $a_0$ ) for three O-terminations, as shown in Fig. 1 and calculated for  $\text{LaMnO}_3$  (this study) and  $\text{BaTiO}_3$ .<sup>20</sup> Electronic shell displacements are given in parentheses,  $\delta_y$ ,  $\delta_z$  are atomic displacements parallel and perpendicular to the (110) surface

Layer	Atom	LMO		BTO	
		$\delta_z$	$\delta_y$	$\delta_z$	$\delta_y$
A-type					
1	O	-8.25 (-13.03)	-9.34 (-8.34)	-11.16 (-15.54)	-6.70 (-2.58)
2	Mn(Ti)	-1.74	-5.03	-1.83 (-1.83)	-5.33 (-5.23)
2	La(Ba)	3.92	-1.26	4.84 (4.95)	-2.21 (-2.20)
2	O	3.62 (2.28)	3.61 (3.67)	4.54 (3.66)	5.90 (5.36)
3	O	8.44 (9.03)	3.53 (3.00)	6.52 (5.32)	5.58 (5.90)
B-type					
1	O	-1.84 (-6.28)	0.0	-2.89 (-3.80)	0.0
2	Mn(Ti)	-4.46	0.0	-6.18 (-6.06)	0.0
2	La(Ba)	7.92	0.0	26.45 (26.35)	0.0
2	O	4.25 (2.61)	0.0	5.89 (4.44)	0.0
3	O	-0.70 (-0.09)	$\pm 0.5 (\pm 2.07)$	-2.30 (-0.68)	$\pm 3.17 (\pm 4.91)$
C-type					
1	O	-6.88 (-11.74)	$\pm 8.61 (\pm 7.73)$	-9.93 (-14.4)	$\pm 6.18 (\pm 2.6)$
2	Mn(Ti)	-2.13	$\pm 5.26$	-3.02 (-3.02)	$\pm 5.87 (\pm 5.77)$
2	La(Ba)	4.29	0.0	5.45 (5.54)	0.0
2	O	1.27 (0.0)	0.0	0.93 (0.18)	0.0
3	O	9.89 (10.61)	$\pm 4.08 (\pm 3.33)$	7.98 (7.11)	$\pm 5.30 (\pm 4.93)$
D-type					
1	O	5.02 (-2.15)	0.0		
2	Mn(Ti)	-6.51	0.0		
2	La(Ba)	2.27	0.0		
2	O	-14.04 (-15.99)	0.0		
3	O	3.95 (3.88)	$\pm 5.60 (\pm 4.87)$		

**Table 4** Surface energies for three different (110) O-terminations shown in Fig. 1, as calculated for LaMnO<sub>3</sub>, SrTiO<sub>3</sub> and BaTiO<sub>3</sub> perovskites. SM-2 and SM-16 refer to the number of relaxed near-surface planes

Termination	SM-2	SM-16
LaMnO <sub>3</sub> -A-type	2.59	2.06
B	4.11	4.06
C	2.80	1.95
D	6.70	6.78
SrTiO <sub>3</sub> -A-type	1.54	0.92
B	3.13	3.31
C	1.63	0.76
TiO	2.21	2.36
Sr	3.04	3.37
BaTiO <sub>3</sub> -A-type	1.58	1.83
B	4.66	4.84
C	1.84	1.82
TiO	2.11	2.36
Ba	3.79	4.16

## IV. Conclusions

In conclusion, we found that the energetically most favourable O-terminated LaMnO<sub>3</sub> surface is that with the “zig-zag” (1 × 2) reconstruction. The A configuration is only slightly higher in energy. In contrast, the symmetrical B configuration is much higher in energy, whereas the configuration D (O ions sitting above the Mn<sup>3+</sup>) is energetically the most unfavourable.

The reconstructed C termination reveals no dipole moment parallel to the surface, but a considerable dipole moment perpendicular to the surface. Note that this surface contains high concentration of O vacancies which remove the macroscopic infinite dipole moment and thus stabilize the surface. The preliminary *ab initio* calculations of this surface are discussed in ref. 34. We observe large polarization of the surface O ions, especially for the case D (O sits atop the Mn ions). In this case the core-shell separation is close to the limit of the applicability of the harmonic approximation, but we are more interested in the semi-quantitative understanding of the surface polarization rather than in very accurate numbers.

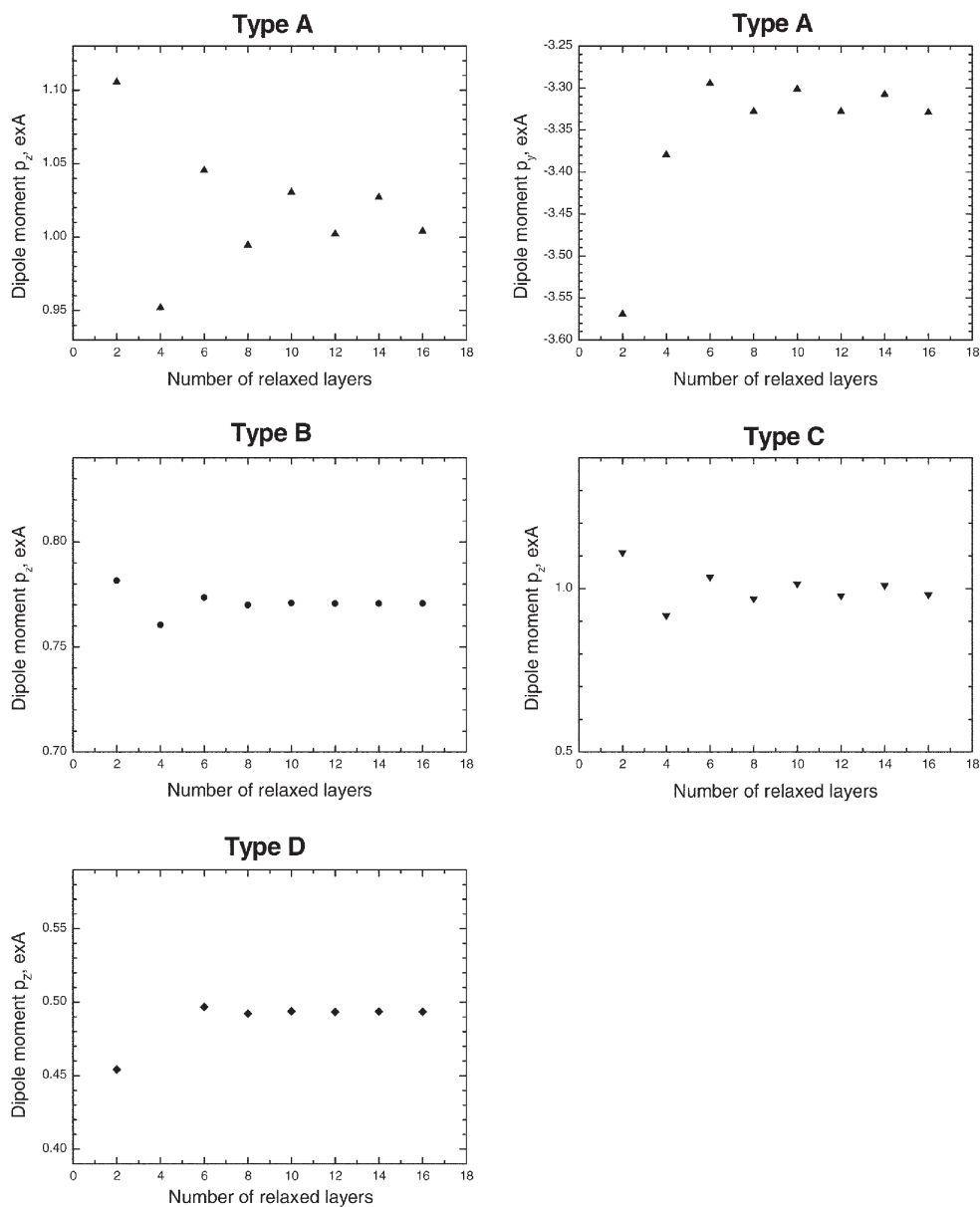


**Fig. 3** Surface polarization and dipole moments perpendicular and parallel to the LaMnO<sub>3</sub> (110) O-terminated surface.

The *ab initio* study estimates the (110) surface relaxation energy as 2.8 eV, in qualitative agreement with 4 eV obtained in this SM study, and confirms also a considerable covalency of the Mn–O bonding. Pattern of atomic displacements for the LaMnO<sub>3</sub> (110) surface is similar to that for iso-structural BaTiO<sub>3</sub> (110) O-termination, the LaMnO<sub>3</sub> shows slightly larger surface energies for the A and C terminations than the BaTiO<sub>3</sub>. Lastly, note that the calculated surface relaxation energies exceed by an order of magnitude those of the Jahn–Teller energy, and even more so, the magnetic effects relevant to the magnetoresistance.<sup>4</sup>

We are well aware of the fact that stability considerations relevant to real conditions also require taking into account adsorbate effects as well as vibrational entropy effects.

## Acknowledgements

This study was partly supported by the German–Israeli Foundation (grant Nr GIF G-703.41.10/2001) and by US Army Research Office (ARO-MURI:DAAD19-01-1-0517). Authors are indebted to R. Evarestov, S. Dorfman, N. Kovaleva and J. Fleig for many fruitful discussions.

## References

- 1 C. Noguera, *Physics and Chemistry at Oxide Surfaces*, Cambridge University Press, New York, 1996.
- 2 J. F. Scott, *Ferroelectric Memories*, Springer, Berlin, 2000.
- 3 J. Fleig, K. D. Kreuer, and J. Maier, in *Handbook of Advanced Ceramics*, ed. S. Somiya, Elsevier, Singapore, 2003, p. 57.
- 4 N. Kovaleva, J. L. Gavartin, A. L. Shluger, A. V. Boris and A. M. Stoneham, *J. Expt. Theor. Phys.*, 2002, **94**, 178.
- 5 J. Padilla and D. Vanderbilt, *Surf. Sci.*, 1998, **418**, 64.
- 6 J. Padilla J and D. Vanderbilt, *Phys. Rev. B*, 1997, **56**, 1625.
- 7 B. Meyer, J. Padilla and D. Vanderbilt, *Faraday Discuss.*, 1999, **114**, 395.
- 8 F. Cora and C. R. A. Catlow, *Faraday Discuss.*, 1999, **114**, 421.
- 9 R. E. Cohen, *Ferroelectrics*, 1997, **194**, 323.
- 10 L. Fu, E. Yaschenko, L. Resca and R. Resta, *Phys. Rev. B*, 1999, **60**, 2697.
- 11 C. Cheng, K. Kunc and M. H. Lee, *Phys. Rev. B*, 2000, **62**, 10 409.
- 12 E. A. Kotomin, R. I. Eglitis, J. Maier and E. Heifets, *Thin Solid Films*, 2001, **400**, 76.
- 13 E. Heifets, R. I. Eglitis, E. A. Kotomin, J. Maier and G. Borstel, *Phys. Rev. B*, 2001, **64**, 235 417.
- 14 E. Heifets, R. I. Eglitis, E. A. Kotomin, J. Maier and G. Borstel, *Surf. Sci.*, 2002, **513**, 211.
- 15 E. Heifets, S. Dorfman, D. Fuks and E. A. Kotomin, *Thin Solid Films*, 1997, **296**, 76.
- 16 E. Heifets, S. Dorfman, D. Fuks, E. A. Kotomin and A. Gordon, *J Phys.: Condens. Matter*, 1998, **10**, L 347.
- 17 D. Fuks, S. Dorfman, E. Heifets, E. A. Kotomin, and A. Gordon, in *Structure and Evolution of Surfaces*, ed. R. C. Cammarata, E. H. Chason, T. L. Einstein and E. D. Williams, Materials Research Society, Pittsburgh, PA, 1997, p. 305.
- 18 S. Dorfman, E. Heifets, D. Fuks, E. A. Kotomin, J. Felsteiner, in *Materials for Smart Systems II*, ed. E. P. George, R. Gotthardt and K. Otsuka, Materials Research Society, Pittsburgh, PA, 1997, p. 219.
- 19 S. Tinte and M. G. Stachiotti, *AIP Conf. Proc.*, 2000, **535**, 273.
- 20 E. Heifets, E. A. Kotomin and J. Maier, *Surf. Sci.*, 2000, **462**, 19.
- 21 A. Filipetti and W. E. Pickett, *Phys. Rev. Lett.*, 1999, **83**, 4184; *Phys. Rev. B*, 2000, **62**, 11 571.
- 22 P. W. Tasker, *J. Phys. C: Solid State Phys.*, 1979, **12**, 4977.
- 23 A. Pojani, F. Finocchi and C. Noguera, *Surf. Sci.*, 1999, **442**, 179.
- 24 A. Stashans and S. Serrano, *Surf. Sci.*, 2002, **497**, 285.
- 25 E. Heifets, R. Eglitis, E. A. Kotomin and W. A. Goddard III, *AIP Conf. Proc.*, 2003, **677**, 210.
- 26 E. Heifets, E. A. Kotomin and P. W. M. Jacobs, *Thin Solid Films*, 2000, **374**, 64.
- 27 Y.-S. Su, T. A. Kaplan, S. D. Mahanti and J. F. Harrison, *Phys. Rev. B*, 2000, **61**, 1324.
- 28 M. Nicastro and C. H. Patterson, *Phys. Rev. B*, 2002, **65**, 205 111.
- 29 M. Cherry, M. S. Islam and C. R. A. Catlow, *J. Solid State Chem.*, 1995, **118**, 125.
- 30 R. A. De Souza, M. S. Islam and E. Ivers-Tiffée, *J. Mater. Chem.*, 1999, **9**, 1621.
- 31 S. M. Woodley, P. D. Battle, C. R. A. Catlow and J. D. Gale, *J. Phys. Chem. B*, 2001, **105**, 6824.
- 32 D. H. Gay and A. L. Rohl, *J. Chem. Soc., Faraday Trans.*, 1995, **91**, 925.
- 33 F. Bottin, F. Finocchi and C. Noguera, *Phys. Rev. B*, 2003, **68**, 35 418.
- 34 R. A. Evarestov, E. A. Kotomin, E. Heifets, J. Maier and G. Borstel, *Solid State Commun.*, 2003, **127**, 367.